MATERIALS PHYSICS AND MECHANICS RESEACH ARTICLE

Submitted: November 29, 2023 Revised: December 12, 2023 Accepted: February 6, 2024

Microstructure, mechanical properties and heat resistance of AL30 piston alloy produced via electromagnetic casting

M.Yu. Murashkin [1] ✉, **L.I. Zainullina** [1], **M.M. Motkov** [2], **A.E. Medvedev** [1], **V.N. Timofeev** [2], **N.A. Enikeev** [1,3]

[1] Ufa University of Science and Technology, Ufa, Russia

[2] Siberian Federal University, Krasnoyarsk, Russia

[3] Saint Petersburg State University, Saint Petersburg, Russia

✉ m.murashkin.70@gmail.com

ABSTRACT

The paper explores the microstructure, mechanical properties and heat resistance of the piston alloy AL30 (AK12MMgN) for the first time produced via continuous casting into an electromagnetic mold (electromagnetic casting, EMC). The study demonstrates that casting into EMC allows for the formation of a homogeneous dispersed microstructure in both the peripheral and central zones of the ingot, consisting of a blend of aluminum's solid solution and eutectic, which contains lamellar silicon (Si). The volume fraction of compact primary Si particles does not exceed 1 %. In addition to Si, the aluminum matrix contains the phases of crystallization origin such as ε-Al_3Ni, π-$Al_8FeMg_3Si_6$, *Q*-$Al_4Cu_2MgSi_7$ and S-Al_2CuMg. The analysis of the evolution of microstructure and properties of a cast alloy after conventional heat treatment (HT) reveals that microstructural changes induced by HT lead to the AL30 alloy having mechanical properties that far exceed the properties of its counterparts obtained through traditional casting methods. The research analysis shows that mechanical properties and heat resistance of the AL30 alloy produced via EMC with subsequent T6 treatment are comparable to the deformable piston alloys such as the AK12D alloy after similar heat treatment.

KEYWORDS

piston aluminum alloy • electromagnetic casting • heat treatment • microstructure• phase composition mechanical properties • heat resistance

Acknowledgements. *M.Yu.M, L.I.Z. and N.A.E. acknowledge the support from the Russian Ministry of Science and Higher Education (state assignment FEUE-2023-0007).*

Citation: Murashkin MYu, Zainullina LI, Motkov MM, Medvedev AE, Timofeev VN, Enikeev NA. Microstructure, mechanical properties and heat resistance of AL30 piston alloy produced via electromagnetic casting. *Materials Physics and Mechanics*. 2024;52(1): 81–94.
http://dx.doi.org/10.18149/MPM.5212024_8

Introduction

Most of the pistons for internal combustion (IC) engines are made of special heat-resistant aluminum piston alloys [1,2]. For example, in Russian Federation, the commonly used materials for pistons produced by permanent mold casting are the eutectic modifications of silumin alloys such as AL25(AK12M2MgN) and AL30(AK12MMgN), which after hardening heat treatment T6 (following the national standard GOST 1583-93 [3]) have the room-temperature strength in the range of 195-235 MPa [1,4]. Likewise, engine pistons abroad are generally manufactured from the M124 alloy (AlSi12CuMgNi), which is similar in chemical composition and properties to the materials produced in Russian

Federation [2]. Following the need to make the IC engines, and therefore their pistons, substantially more efficient, one of the timely research trends in this field deals with increasing the mechanical and service properties of silumin piston alloys. Due to the fact that strength, ductility and heat resistance are structure-dependent features, nowadays, much attention is focused on the formation of microstructure in piston materials, which will ensure the maximum level of properties. As is known, decreasing dendritic cell size of the aluminum solid solution, as well as the refinement of the second phases included in the eutectic may result in a higher complex of properties of cast alloys [2,5]. Nowadays, such changes in microstructure are achieved by modifying the alloy composition during casting [1,2,6–9], by using casting or powder metallurgy techniques that ensure high crystallization rates [10–12], by using various types of heat [13] and deformation treatments [14,15], including severe plastic deformation [16–18].

Recently, much attention has been focused on the fabrication of semifinished products from aluminum alloys in the form of bars of small cross-section (diameter from 8 to 12 mm) by continuous electromagnetic casting method (EMC). During EMC, intensive melt circulation in the region of ingot crystallization is implemented, which promotes the formation of a homogeneous microstructure throughout its volume, and the high cooling rate (10^3-10^5 K/s) ensures the formation of highly dispersed cast structures [19–22]. In addition, high cooling rate during crystallization leads to abnormal supersaturation of aluminum with alloying elements [19,20]. All the above-listed microstructural features of cast rods produced by EMC favorably influences their mechanical and service properties after various deformation or deformation-thermal treatments [19–22]. As was demonstrated recently in the work [23] on the example of the formation of the solid solution in the Al-Zn-Mg-Ca-Fe system alloy, the EMC method may be used to produce bulk cylindrical billets with a homogeneous structure in which the dendritic cell size is less than 10 μm and the second phases are less than 3 μm in size.

Herein, we study the microstructure features, mechanical properties and heat resistance of a solid cast rod from piston alloy AL30, that was for the first time produced through casting in EMC subsequently conventionally hardened by heat treatment.

Materials and Methods

The experiments were conducted on the AL30 (AK12MMgN) alloy bar with a diameter of 80 mm obtained by continuous casting in EMC at the Research and Production Center of Magnetic Hydrodynamics Ltd [24]. The alloy was produced on the basis of primary aluminum grade A85 (not less than 99.85 wt. % Al), silicon grade KR00 (not less than 99.41 wt. % Si), magnesium grade MG-95 (not less than 99.95 wt. % Mg), copper grade M00k (not less than 99.9 wt. % Cu), and alloying compositions AlNi20 and AlSr10. Prior to casting, the finished melt was degassed with argon and simultaneously treated with a special flux. Continuous casting in the EMC unit was carried out at a temperature of 750 °C and rate of 5 mm/s. Chemical composition of the peripheral and central zones of the cast rod was observed using the Bruker Q4 Tasman optical emission spectrometer and is given in Table 1. As is seen, the chemical composition of the rod obtained by casting in EMC does not change from the periphery to its central zone and fully meets the requirements of the GOST 1583-93 national standard [3].

Table 1. Chemical composition of the alloy AL30 (wt. %)

	Si	Cu	Mg	Ni	Fe	Ti	Cr	Mn	Zn	ΣSn, Pb
A	13.1/13.0*	1.3/1.3	1.0/1.0	1.3/1.3	0.25/0.20	<0.2				<0.06
B	11-13	0.8-1.5	0.8-1.3	0.8-1.3	≤0.7	≤0.2				≤0.06

A – chemical composition of the alloy AL30 produced by electromagnetic casting
B – chemical composition of the alloy AL30 [3]
* - chemical composition of the peripheral/central zone of the cast rod

The microstructure and properties of the cast rod were examined precisely in the peripheral (the area of these parts was determined by the data of structural analysis) and central parts of the rod. The choice of such areas for study was determined by the fact that in the process of producing the cast rod by EMC, there was observed the maximum difference in the rate of material crystallization between these areas and, therefore, the different degree of dispersion of the obtained microstructure.

One part of the samples from the peripheral and central zones of the cast rod was subjected to heat treatment (HT) T1, the other part was subjected to heat treatment T6, according to the regimes recommended in [3] for the AL30 alloy. The T1 treatment included artificial aging at a temperature of 190 °C for 12 hours (without preliminary hardening). The T6 treatment included annealing at 520 °C for up to 4 hours, quenching into water and aging at 180 °C, 6 hours.

After the T6 treatment, the AL30 alloy samples were used for the examination of heat resistance according to the method introduced in [25]. The samples were annealed at a temperature of 300 °C and 100 hours of holding time. Samples of the AK12D alloy in the T6 state were subjected to similar annealing. During annealing, intermediate measurements of hardness change after 1, 3, 5, and 24 hours of exposure were made.

HT and annealing of the samples to determine the heat resistance of the alloy were carried out in a chamber furnace Nabertherm N15/65HA.

The microstructure was examined using optical microscopy (OM), scanning and transmission electron microscopy (SEM and TEM), and X-ray diffraction analysis (XRD).

OM was performed on an Olympus QX 51 microscope. SEM was performed on a Tescan Mira scanning microscope at 10-20 kV accelerating voltage. Chemical composition of the second phases was analyzed by energy dispersive X-ray spectroscopy (EDS) using the INCA X-Act installation from Oxford instruments. SEM was performed on a JEOL JEM 2100 transmission microscope at 200 kV accelerating voltage. The samples for microstructure studies were prepared by jet electrolytic polishing of thin foils on a Tenupol-5 equipment from Struers Inc. in a solution of 20 % nitric acid and 80 % methanol at ≥ -20 °C and 10-20 V voltage. ImageJ software and Grain Size software package were used to process the obtained images and quantitatively analyze the microstructure features (average dendritic cell size, average section size of the second phase within the eutectic/size of second phase particles, volume fraction of particles).

X-ray diffraction analysis of the samples was performed on a Bruker D8 Discover diffractometer using the Cu-Kα-radiation. The results were used to determine the phase composition and lattice period (*a*) of the samples in different zones of the cast rod and after HT. The *a* value was calculated using the Rietveld method and MAUD software [26].

Vicker's microhardness [27] was measured using an EMCO-Test DuraScan-50 device at a load of 1 H and a dwell time of 15 s.

Mechanical properties (conditional yield stress ($\sigma_{0,2}$), ultimate tensile strength (σ_{UTS}) and elongation to failure (δ_5)) after HT were determined using the results of static tensile tests, which were performed on an Instron 5982 universal testing machine in accordance with the GOST 1497-84 national standard [28].

Results and discussion

Microstructure of the alloy after casting into EMC mold and subsequent heat treatment

Typical microstructure of the AL30 alloy in the peripheral and central parts of the cast rod produced by EMC is shown in Fig. 1(a,b). The microstructure is composed of dendrites of aluminum solid solution (α_{Al}) and the eutectic, with dispersed lamellar silicon (Si) located along the α_{Al} boundaries (Figs. 2 and 3). In addition to Si, the particles that are different in color from it were noted in the eutectic. Also, a small amount of coarse compact particles of primary Si were observed in the microstructure of the cast rod - both in the peripheral and central zones (Fig. 1(a,b)).

General view of the microstructure of the AL30 alloy obtained by casting into EMC resembles the eutectic silumins produced by conventional casting methods [1,2,4–6]. However, the size of cells and of lamellar silicon included in the eutectic, especially in the peripheral zone, indicates an unusually high cooling rate of the melt during its crystallization. Quantitative evaluation of the cross-sectional area of the bar demonstrated that the microstructure, which is characteristic of the peripheral zone (Fig. 1(a)), occupies about 20 % of its total area.

The results of quantitative analysis of microstructure in the cast rod are presented in Table 2.

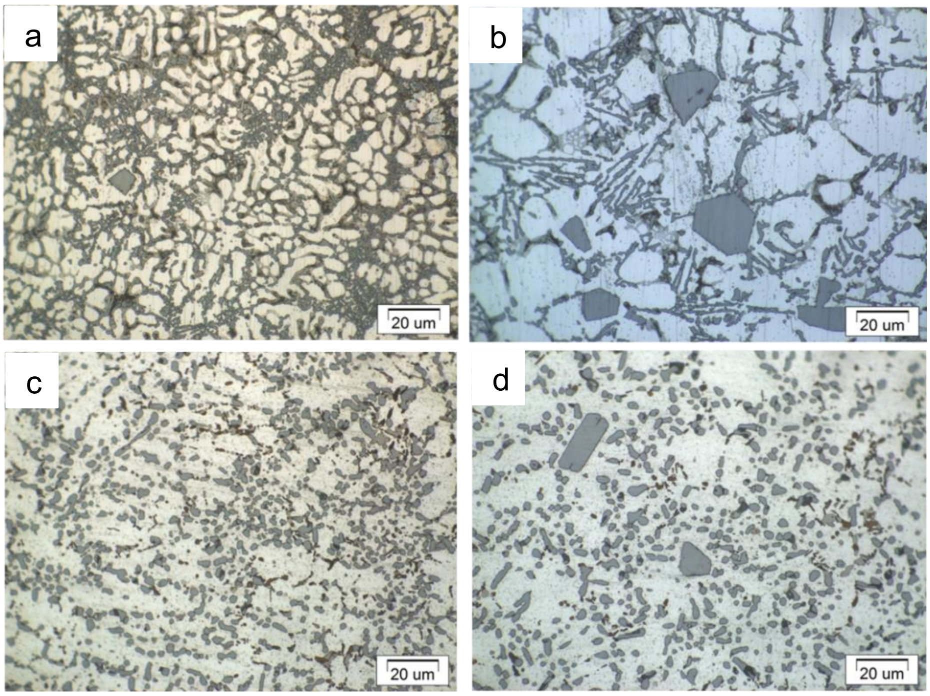

Fig. 1. Microstructure of the AL30 alloy cast rod after casting into EMC (a, b) and after T6 treatment (c, d). (a, c - peripheral zone of the rod; b, d - central zone of the rod) (OM method)

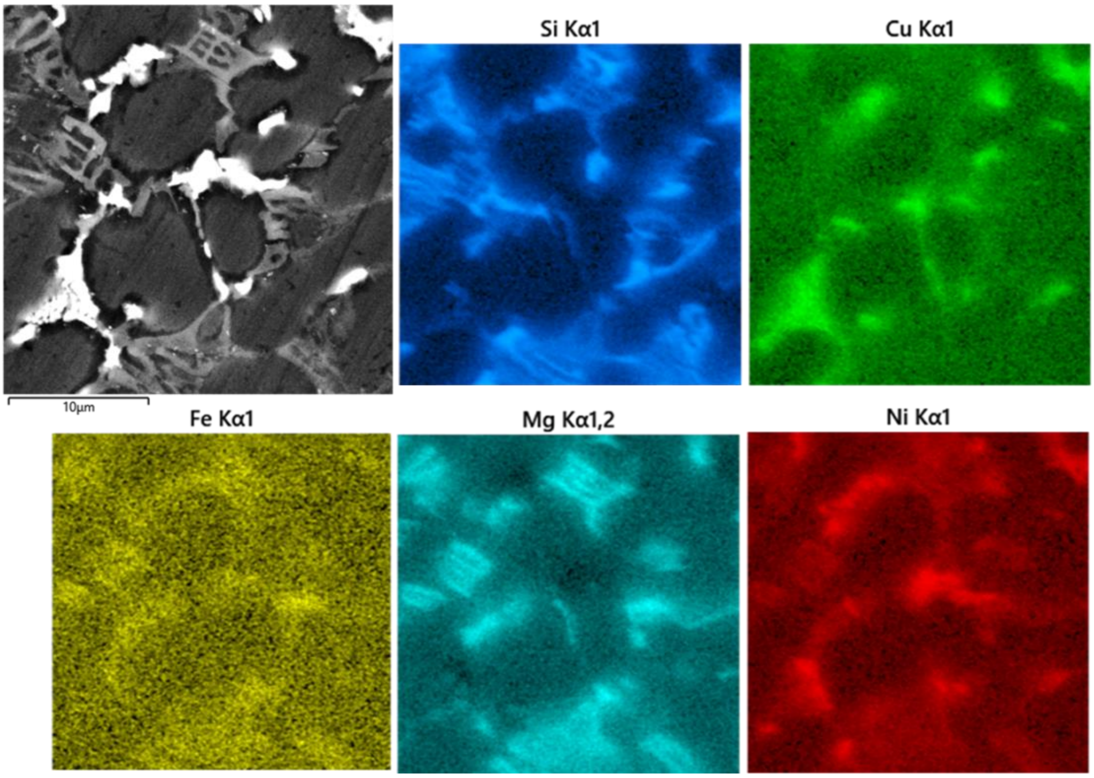

Fig. 2. Typical microstructure area in the peripheral zone of the cast rod and elemental mapping of such area (SEM)

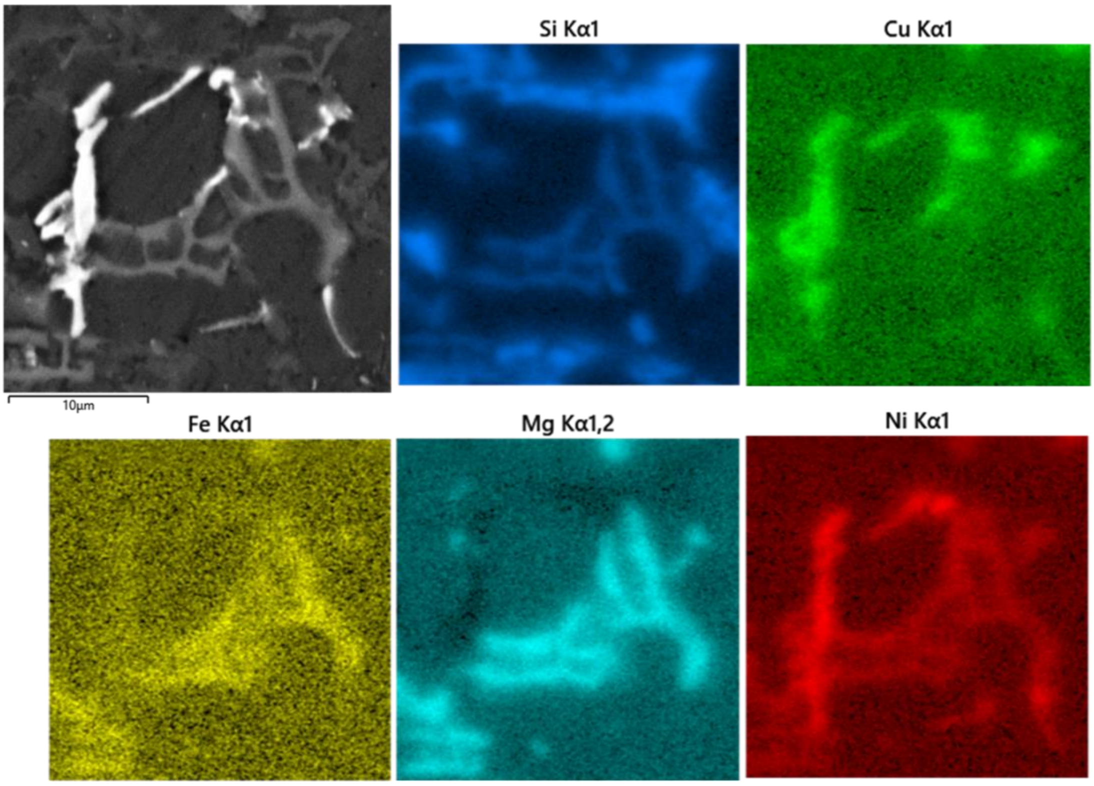

Fig. 3. Typical microstructure area in the central zone of the cast rod and elemental mapping of such area (SEM)

Table 2. Microstructural characteristics of the alloy AL30 alloy after casting into EMC and subsequent T6 treatment

State	Zone of cast rod	*d*, μm	d_{Si}, μm	Q_{Si}, %	*h*, μm	K_f	Q_V, %
EMC	Periphery	7.6 ± 0.4	11.3 ± 0.5	0.3 ± 0.1	0.96 ± 0.12	-	24 ± 3
	Center	16.6 ± 0.6	16.2 ± 0.4	1.1 ± 0.1	1.57 ± 0.16	-	22 ± 5
T6	Periphery	-	-	-	2.80 ± 0.28*	2.1	25 ± 4
	Center	-	-	-	5.65 ± 1.45*	2.7	23 ± 3

where *d* is an average size of dendritic cell; d_{Si} and Q_{Si} are average size and volume fraction of primary Si particles; *h* is average size of second phase section inside eutectic; K_f is mold ratio of second phase particles; Q_V is volume fraction of second phase particles; * average size of second phase particles

The obtained data reveals that the sizes of dendritic cells formed by α_{Al} and eutectic are more than twice smaller in the peripheral zone of the cast rod. Also in this zone, the cross-section of Si plates included in the eutectic is noticeably smaller than the cross-section of Si plates formed in the central zone. As is known, the increase in the crystallization rate (V_c) reduces not only the size of dendritic cells (*d*), but also the size of second phase particles [5]. At the same time, the dependence between *d* and V_c has a linear character on a logarithmic scale and persists up to cooling rates ⩾ 10^8 K/s. According to this dependence, in the peripheral and central zone of the cast rod of AL30 alloy, the value V_c differs by more than an order of magnitude, constituting ⩾ 10^3 and ⩽10^2 K/s, respectively. It is the difference in V_c that explains the differences revealed in the microstructure (Table 2). The microstructure formed in the peripheral zone is qualitatively similar to the microstructure formed in cast billets of aluminum alloys for electrical and structural purposes, which were also obtained by casting into EMC [19–22]. The microstructure in the central zone of the cast rod is similar to the microstructure that was obtained in eutectic silumin piston alloys by casting methods, the latter providing a noticeably lower V_c [1,2,4–6]. However, considering the results of study of crystallization in a bulk rod of the alloy Al-Zn-Mg-Ca-Fe during casting into EMC, the values of V_c still remain high and may reach 600 K/s [23].

Considering the different color of particles, which is clearly visible in Figs. 1-3, the eutectic composition includes other phases in addition to Si. Distribution maps in the areas of the peripheral and central zones of the cast rod for the main alloying elements made by EDS (Fig. 2 and 3) showed the presence of Si and Mg in addition to aluminum in the dark gray plates include, and the presence of Cu, Ni and Fe in the light gray phases.

The results of X-ray phase analysis are presented in Fig. 4 and the data made it possible to determine the phase composition of the alloy. The phases ε-Al_3Ni, π-$Al_8FeMg_3Si_6$, *Q*-$Al_4Cu_2MgSi_7$ and S-Al_2CuMg were formed both in the peripheral and central parts of the cast rod in addition to Si during casting into EMS. The presence of these phases has been previously reported in similar silumin piston alloys [5,6,29,30].

The absence of noticeable differences in the value of lattice parameter in the peripheral and central parts of the cast rod, which constitutes 4.0487 ±0.0001 and 4.0490 ± 0.0001 Å respectively, means that the concentration of alloying elements in α_{Al} after EMC is almost similar.

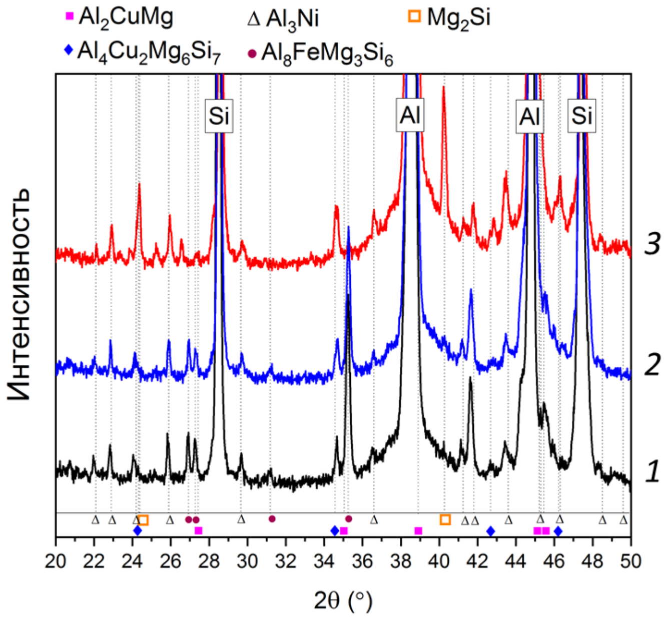

Fig. 4. X-ray profiles of the sample of AL30 alloy cast rod obtained from the peripheral (*1*) and central (*2*) zones, as well as from the central zone after T6 treatment (*3*) (X-ray analysis)

When T1 heat treatment was performed, the AL30 alloy samples were subjected only to artificial aging at a temperature that could not lead to significant changes in the size and morphology of the second phases [5,29]. Therefore, microstructure evolution in the cast rod was examined after T6 heat treatment. Typical images of the microstructure after such treatment in the peripheral and central parts of the rod are presented in Fig. 1(c,d), as well as in Figs. 5-7.

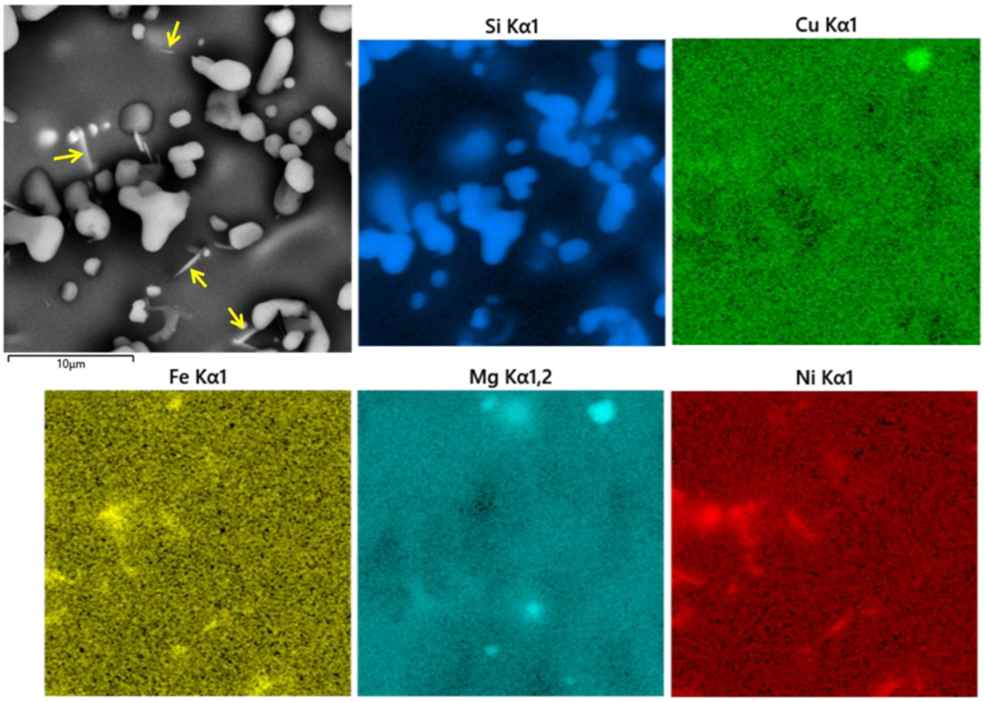

Fig. 5. Typical microstructure area in the peripheral zone of the cast rod and elemental mapping of such area (SEM)

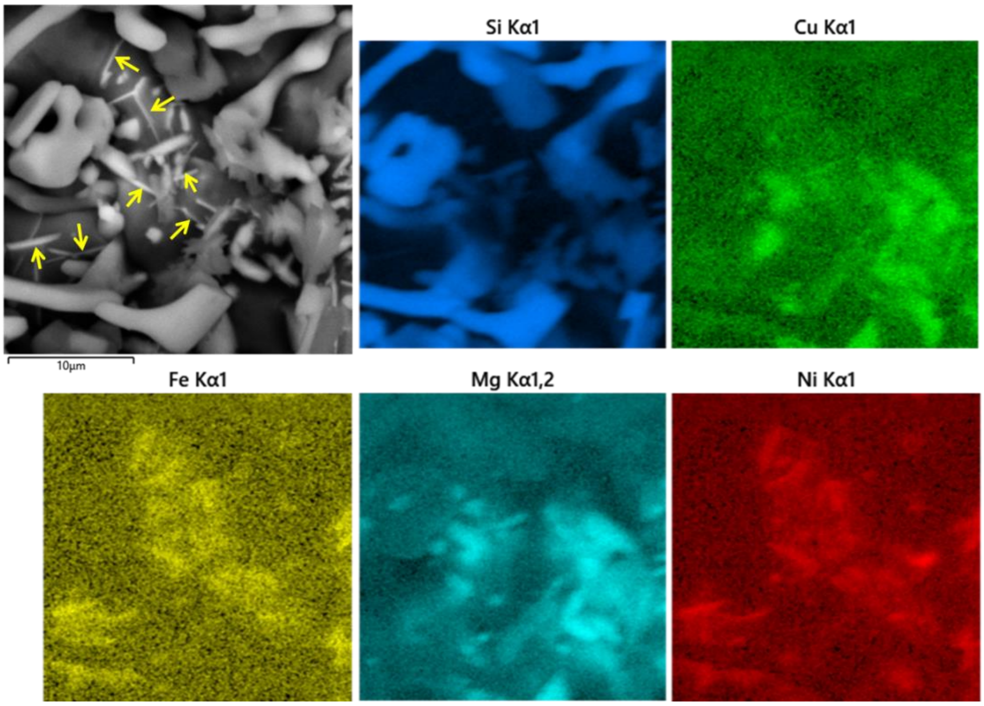

Fig. 6. Typical microstructure area in the central zone of the cast rod and elemental mapping of such area (SEM)

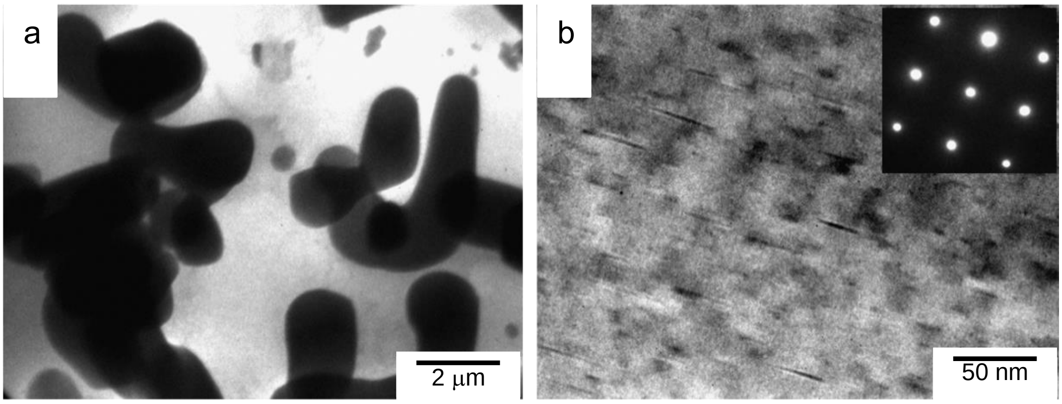

Fig. 7. Microstructure in the peripheral zone of the cast rod after T6 treatment: (a) after annealing at 520 °C and quenching; (b) after quenching and artificial aging (axis of the microdiffraction pattern zone [001]) (TEM)

As can be seen, after T6 treatment at the stage of annealing at 520 °C, fragmentation and spheroidization of lamellar Si and other phases in the eutectic occurred. In addition, the results of quantitative analysis (Table 2) demonstrate that annealing leads to coarsening of the particles (coalescence). However, there is still a noticeable difference in the particle size in the peripheral and central parts, which was noted earlier for the cast rod before HT.

In addition to the particles, whose morphology and size changed as a result of annealing at 520 °C, the microstructure of the alloy exhibits the presence of particle in the form of thin plates/needles with a smooth surface (indicated by arrows in Figs. 5 and 6), which did not undergo fragmentation. Elemental mapping showed that these particles, in addition to aluminum, include Fe and Ni. As was stated in the work [29], the particles of phases with similar morphology, which include alloying elements of a low solubility in aluminum, possess high resistance to thermal effects. Such particles include the particles of ε-phase (Al_3Ni), which was possible to identify by X-ray diffraction, as well as, probably, the particles of Al_9FeNi – the presence of a small amount of such phase in the alloy is indicated by EDS results.

After the second stage of T6 treatment, which is artificial aging, the formation of rod-/plate-like particles of secondary phase is observed in the aluminum matrix, which are oriented in a strictly defined direction, have a thickness of several nanometers and a length in the range from 20 to 100 nm (Fig. 7(b)). The XRD data reveals a new well-defined diffraction peak related to the Mg_2Si phase that develops on X-ray diffraction pattern *3* (Fig. 4) after T6 heat treatment. According to [31], the particles of this phase develop after artificial ageing in the form of thin plates lying in $\{100\}_{Al}$ planes, i.e., as in the image shown in Fig. 7(b). After T6 treatment, the lattice parameter of the alloy was as close as possible to that of pure aluminum (4.0507 ± 0.0001 Å). Such a change in the lattice parameter indicates the process of decomposition of α_{Al} as a result of aging and that aluminum solid solution has reached the maximum depletion of alloying elements. It is known that in silumins, as a result of heat treatment, including aging, other strengthening phases such as Al_2Cu, Al_2CuMg, and secondary Si can be formed in addition to Mg_2Si [29]. However, such phases were not detected in the examined samples in the process of microstructural analysis either by TEM or XRD. The possibility of detecting the phases of such composition might be limited by research techniques applied in the present study.

It should be noted that the microstructure that was formed in the AL30 alloy due to continuous casting into EMC and subsequent T6 heat treatment is close in its parameters to the microstructure of piston alloys with a similar chemical composition, which are used for manufacturing of semifinished products using deformation processing [14–18]. In the peripheral zone of the cast rod, in which Vc ⩾ 10^3 K/s was implemented after HT, it was possible to form a more dispersed microstructure. Similar microstructure was observed in the billets subjected to severe plastic deformation [16–18] or obtained by selective laser melting (SLM), in the process of which, as in the case of EMC casting, V_c in the range of 10^4-10^7 K/s is realized [11,12].

Mechanical properties of the alloy after heat treatment

Mechanical properties of the cast rod obtained by casting into EMC from the alloy AL30 and subsequent T1 and T6 heat treatment are presented in Table 3. In addition, Table 3 lists the properties of counterparts produced by conventional casting into the steel coquille (i.e., permanent mold casting) in Russian Federation [2,25] and abroad [3]. For comparison, the properties of semifinished products made of piston alloys similar in chemical composition, which were obtained using the deformation processing techniques, including severe deformation by equal-channel angular pressing (ECAP) [17], as well as by SLM technology [11,12], are also presented.

The data summarized in Table 3 from the present as well as previously carried out studies clearly demonstrate that the samples of cast rod obtained by casting into EMC from the alloy AL30 after T1 and T6 treatments are considerably superior to the mechanical properties of counterparts obtained by conventional casting. After T6 treatment the alloy AL30 demonstrates the "strength-ductility" ratio at the level of forged piston alloy M124R(AlSi12CuMgNi) [2] and alloy Al-11Si processed by ECAP [17], as well as of deformable alloy AK12D. However, its strength is found to be inferior to the alloys produced by SLM technology [11,12].

Table 3. Mechanical properties of the cast rod obtained from the alloy AL30 after conventional HT and of eutectic silumins with close chemical composition manufactured by different techniques

Alloy	State	Cast rod zone	*HV*	σ_{UTS}, MPa	$\sigma_{0.2}$, MPa	δ_5, %
AL30 (AK12MMgN)	T1	Periphery	135 ± 5	345 ± 10	250 ± 15	2.1 ± 0.3
		Center	139 ± 9	309 ± 5	295 ± 7	0.5 ± 0.1
	T6	Periphery	150 ± 4	404 ± 5	335 ± 8	4.2 ± 0.3
		Center	147 ± 9	393 ± 7	329 ± 9	2.4 ± 0.3
	T1 [3]	-	HB90	196	-	0.5
	T6 [3]	-	HB100	216	-	0.7
AL25 (AK12M2MgN)	T6 [25]	-	-	360	-	-
M124 (AlSi12CuMgNi)	T6 [2]	-	-	200-251	190-230	< 1
M124R (AlSi12CuMgNi)	T6 [2]	-	-	300-370	280-340	< 1
AK12D*	T6	-	156 ± 5	407 ± 4	387 ± 6	1.9 ± 0.2
Al-11Si	ECAP +T6 [17]	-	-	~ 390	-	~ 7
Al10SiMg	SLM [11]	-	-	475	294	2.4
Al-12Si	SLM [12]	-	-	⩾ 425	⩾ 275	⩾ 6
* – heat treatment and tests were carried out in the framework of present study						

The level of properties displayed by the alloy AL30, obtained by casting into EMC and subjected to HT, is in good agreement with its microstructural features. In terms of dispersibility, the alloy AL30 is close to the alloys that undergo deformation treatment and occupies an intermediate position between the counterparts obtained by conventional casting methods and those produced by SLM technology. The increased strength of SLM-produced alloys relates to their ability to form a highly dispersed structure, which surpasses the structure resulting from casting into EMC, including the structure in the peripheral zone of the cast rod obtained from the alloy AL30. For example, as was demonstrated in the work [11], the samples of SLM-produced alloy $Al_{10}SiMg$ revealed the formation of a microstructure featuring dendritic cells of submicron scale (around 500 nm) and Si particles in the nanometer range.

Evaluation of heat resistance of the alloy after casting into EMC and subsequent heat treatment

Traditionally, pistons in IC engines are operated for extended periods (over 1000 hours) at temperatures up to and including 300 °C [1,2]. In this case, it seems important to determine the level at which the strength properties of piston materials become stable under these conditions. For this purpose, it was proposed in [25] to evaluate heat resistance by examining the piston alloys' hardness after annealing at 300 °C for 100 hours. Temperature exposure for the same period is used to determine the long-term strength of such materials.

Table 4 displays the results of evaluation of hardness change in the alloy AL30 samples after T6 heat treatment as a result of annealing at 300 °C. For comparison, the annealing treatment was performed on a sample of deformable alloy AK12D in the state T6, which has a similar chemical composition and level of mechanical properties (Table 3). In addition, Fig. 8 shows the graph of change in hardness with annealing time at 300 °C.

Table 4. Hardness of cast rod obtained from the alloy AL30 after thermal exposure at 300 °C

Rod zone	Initial hardness	Annealing time, h				
		1	3	5	24	100
Periphery	150 ± 4	114 ± 7	98 ± 5	89 ± 4	72 ± 4	66 ± 7
Center	147 ± 8	115 ± 5	98 ± 4	86 ± 5	71 ± 4	68 ± 7

As follows from Table 4 and Fig. 8, the character of hardness change is the same for the peripheral and central parts of the alloy AL30 cast rod. After 1-hour exposure at 300 °C, the sample hardness decreases by ~ 25 %, and hardness values continue to decrease significantly during 24 hours of annealing. Further increase of exposure time does not lead to considerable changes in hardness. It becomes stable at the level of ~ HV70, which is ~ 45 % of the initial hardness - after T6 heat treatment (Table 4). In the work [25], after similar annealing, the samples of alloy AL25 (AK12M2MgN) with close chemical composition, obtained by casting with crystallization under pressure and subjected to T6 treatment, demonstrated residual hardness of about 40 % of the initial hardness, and the samples of deformable alloy AK12D in the T6 state – 47 % (Fig. 8).

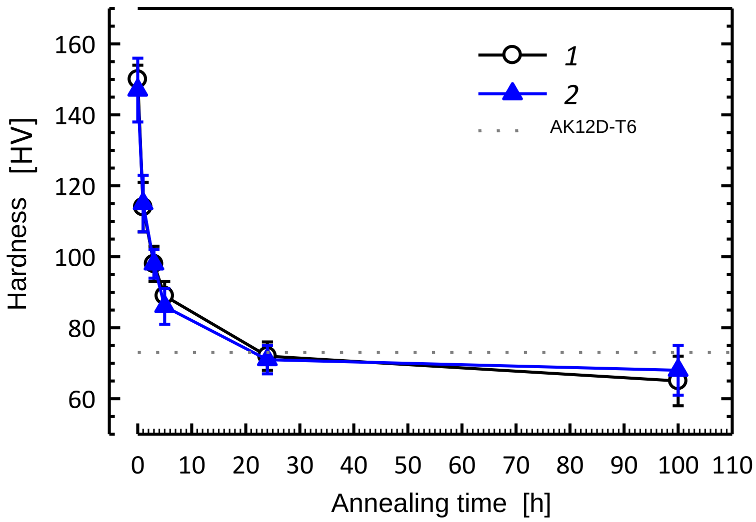

Fig. 8. Change in hardness of the alloy AL30 cast rod after T6 heat treatment with exposure time during annealing 300 °C: (1) – peripheral and (2) – central zones

Based on the analysis of the data herein and previous studies, it may be concluded that the cast rods, obtained from the alloy AL30 by casting into EMC and subsequent T6 heat treatment, exhibit heat resistance at the level of counterparts produced by casting or deformation processing. The absence of difference in the heat resistance level in different zones of the alloy AL30 cast rod might relate to the fact that the sizes of Si particles and other secondary phases are insufficient for more pronounced stabilization of strength characteristics under extended thermal exposure (at 300 °C).

First results obtained in this study have shown that the use of continuous casting into EMC in combination with conventional HT to produce bulk billets of piston eutectic silumins makes it is possible to increase their mechanical properties while maintaining heat resistance at a high level. However, more research is needed to study the potential for further increasing the complex of properties through the formation of more homogeneous and dispersed structures (at submicron and/or nanoscale level) as well as improving the conditions of casting into EMC and HT modes.

Conclusions

1. The microstructure, mechanical properties and heat resistance of piston alloy AL30 (AK12MMgN), which for the first time was obtained by continuous casting into an electromagnetic mold (EMC), were studied.
2. It was shown that the EMC technique makes it possible to form a homogeneous dispersed microstructure comprised of a mixture of aluminum solid solution and eutectic with lamellar silicon (Si), as well as secondary phases, including ε-Al_3Ni, π-$Al_8FeMg_3Si_6$, Q-$Al_4Cu_2MgSi_7$ and S-Al_2CuMg, in both the central and peripheral regions of the bulk ingot.
3. It was established that in the alloy AL30, a microstructure formed by casting into EMC with subsequent T6 heat treatment provides the achievement of mechanical properties ($\sigma_{0.2}$, σ_{UTS} and δ_5 not less than 330, 390 MPa and 2.5 % respectively), which are noticeably higher than the properties of its material counterparts produced by conventional casting in Russian Federation and abroad.
4. It was shown that the mechanical properties and heat resistance of the EMC-produced alloy AL30 with subsequent T6 heat treatment are identical to the properties of deformable piston alloys subjected to similar HT.

References

1. Belov NA, Belov VD, Savchenko SV. *Piston silumins*. Moscow: Ore and Metals; 2011. (In-Russian)
2. MAHLE GmbH (Ed.). *Pistons and engine testing*. Stuttgart, Germany: Springer; 2016.
3. Gosstandart of Russia. GOST 1583–93. *Alloys aluminum casting. Specifications*. 1993. (In-Russian)
4. Vyrubov DN, Efimov SI, Ivashchenko NA. *Internal Combustion Engines: Design and Strength Calculation of Piston and Combined Engines*. Moscow: Mashinostroenie Publishing House; 1984. (In-Russian)
5. Zolotorevskiy VS, Belov NA. *Metallurgy of cast aluminum alloys*. Moscow: MISIS Publishing House: 2005. (In-Russian)
6. Kolonakov AA, Kukharenko AV, Deev VB, Abaturova AA. Structure and Chemical Composition of the AK12MMgN Piston Alloy Fabricated Based on Various Charges. *Izvestiya. Non-Ferrous Metallurgy*. 2015;3: 49–55. (In-Russian)
7. Zhang X, Zhou Y, Zhong G, Zhang J, Chen Y, Jie W, Schumacher P, Li J. Effects of Si and Sr elements on solidification microstructure and thermal conductivity of Al–Si-based alloys. *Journal of Materials Science*. 2022;57: 6428–6444.
8. Ganesh K, Hemachandra Reddy K, Sudhakar Babu S, Ravikumar M. Study on microstructure, tensile, wear, and fracture behavior of A357 by modifying strontium (Sr) and calcium (Ca) content. *Materials Physics and Mechanics*. 2023;51(2): 128–139.
9. Kaiser MS. Effect of Solution Treatment on Age-Hardening Behavior of Al-12Si-1Mg-1Cu Piston Alloy with Trace-Zr Addition. *Journal of Casting & Materials Engineering*. 2018;2(2): 30–37.

10. Kumai S. Tear toughness evaluation of high-quality squeeze-cast and rheocast aluminum alloy castings. *Materials Science Forum*. 2006;519-521: 1733–1740.
11. Marola S, Manfredi D, Fiore G, Poletti M.G, Lombardi M, Fino P, Battezzati L. A comparison of Selective Laser Melting with bulk rapid solidification of AlSi10Mg alloy. *Journal of Alloys and Compounds*. 2018;742: 271–279.
12. Takata N, Liu M, Kodaira H, Suzuki A, Kobashi M. Anomalous strengthening by supersaturated solid solutions of selectively laser melted Al–Si-based alloys. *Additive Manufacturing*. 2020;33: 101152.
13. Sjolander E, Seifeddine S. Review. The heat treatment of Al–Si–Cu–Mg casting alloys. *Journal of Materials Processing Technology*. 2010;210: 1249–1259.
14. Hu HE, Wang X, Deng L. High temperature deformation behavior and optimal hot processing parameters of Al-Si eutectic alloy. *Materials Science and Engineering A*. 2013;576: 45–51.
15. Yu SB, Kim MS. Microstructure and High Temperature Deformation of Extruded Al-12Si-3Cu-Based Alloy. *Metals*. 2016;6: 32.
16. Cepeda-Jimenez CM, Garcia-Infanta JM, Zhilyaev AP, Ruano OA, Carreno F. Influence of the supersaturated silicon solid solution concentration on the effectiveness of severe plastic deformation processing in Al–7 wt.% Si casting alloy. *Materials Science and Engineering A*. 2011;528: 7938–7947.
17. Ma F, Takagi M, Saito N, Iwata H, Nishida Y, Suzuki K, Shigematsu I. Tensile properties of an Al–11 mass%Si alloy at elevated temperatures processed by rotary-die equal-channel angular pressing. *Materials Science and Engineering A*. 2005;408: 147–153.
18. Damavandi E, Nourouzi S, Rabiee SM, Jamaati R, Szpunar JA. Effect of route BC-ECAP on microstructural evolution and mechanical properties of Al–Si–Cu alloy. *Journal of Materials Science*. 2021;56: 3535–3550.
19. Belov N, Murashkin M, Korotkova N, Akopyan T, Timofeev V. Structure and properties of Al-0.6 Wt.%Zr wire alloy manufactured by direct drawing of electromagnetically cast wire rod. *Metals*. 2020;10(6): 769.
20. Belov N, Akopyan T, Korotkova N, Murashkin M, Timofeev V, Fortuna A. Structure and properties of Ca and Zr containing heat resistant wire aluminum alloy manufactured by electromagnetic casting. *Metals*. 2021;11(2): 236.
21. Medvedev AE, Zhukova OO, Fedotova DD, Murashkin MYu. The mechanical properties, electrical conductivity, and thermal stability of a wire made of Al–Fe alloys produced by casting into an electromagnetic crystallizer. *Frontier Materials & Technologies*. 2022;3: 96–105.
22. Korotkova NO, Belov NA, Timofeev VN, Motkov MM. Cherkasov S.O. Influence of Heat Treatment on the Structure and Properties of an Al-7% REM Conductive Aluminum Alloy Casted in an Electromagnetic Crystallizer. *Physics of Metals and Metallography*. 2020;121(2): 173–179.
23. Gamin YV, Belov NA, Akopyan TK, Timofeev VN, Cherkasov SO and Motkov MM. Effect of Radial-Shear Rolling on the Structure and Hardening of an Al–8%Zn–3.3%Mg–0.8%Ca–1.1%Fe Alloy Manufactured by Electromagnetic Casting. *Materials*. 2023;16(2): 677.
24. *RPC of Magnetic Hydrodynamics Ltd*. Available from: http://www.npcmgd.com [Accessed 29th November 2023].
25. Vasenin VI. Determining the High-Temperature Strength of Aluminum Alloys. *Metallurgy of Machinery Building*. 2004;3: 38–40. (In-Russian)
26. Lutterotti L, Matthies S, Wenk HR, Schultz A, Richardson J. Combined texture and structure analysis of deformed limestone from time-of-flight neutron diffraction spectra. *Journal of Applied Physics*. 1997;81: 594–600.
27. International Standard Organization. ISO 6507-1:2023. *Metallic materials. Vickers hardness test. Part 1: Test method*. ISO; 2023.
28. Gosstandart of Russia. GOST 1497-84. *Metals. Methods of tension test*. 1986.
29. Belov NA. *Phase composition of industrial and promising aluminum alloys: monograph*. Moscow: MISIS Publishing House; 2010. (In-Russian)
30. Khalikova GR, Kalshchikov RV, Shvets KS, Trifonov VG. Structure and mechanical properties of aluminum alloy AK12MMgN reinforced with SiC particles. *Fundamental Problems of Modern Materials Science*. 2015;12(4): 459–463. (In-Russian)
31. Edwards GA, Stiller K, Dunlop GL, Couper MJ. The precipitation sequence in Al–Mg–Si alloys. *Acta Materialia*. 1998;46(11): 3893–3904.

About Authors

Maxim Yu. Murashkin Sc
Candidate of Technical Sciences
Senior Researcher (Ufa University of Science and Technology, Ufa, Russia)

Lily I. Zainullina Sc
Candidate of Technical Sciences
Associate Professor, Senior Researcher (Ufa University of Science and Technology, Ufa, Russia)

Mikhail M. Motkov Sc
Candidate of Technical Sciences
Senior Researcher (Siberian Federal University, Krasnoyarsk, Russia)

Andrey E. Medvedev Sc
Candidate of Physical and Mathematical Sciences
Senior Researcher (Ufa University of Science and Technology, Ufa, Russia)

Viktor N. Timofeev Sc
Doctor of Technical Sciences
Professor (Siberian Federal University, Krasnoyarsk, Russia)

Nariman A. Enikeev Sc
Doctor of Physical and Mathematical Sciences
Leading Researcher (Ufa University of Science and Technology, Ufa, Russia)
Leading Researcher (Saint Petersburg State University, Saint Petersburg, Russia)